Temperature-triggered reversible micellar self-assembly of linear–dendritic block copolymers†

Hyung-il Lee, Jung Ah Lee, Zhiyong Poon and Paula T. Hammond*

Received (in Cambridge, UK) 6th May 2008, Accepted 27th June 2008
First published as an Advance Article on the web 18th July 2008
DOI: 10.1039/b807561a

Polymeric micelles based on a thermoresponsive linear–dendritic block copolymer were completely disrupted into unimers upon cooling the solution to a temperature below its LCST and reversibly regenerated upon heating again.

There has been considerable interest in controlling nanostructured molecular self-assembly of double-hydrophilic block copolymers (DHBCs) by external stimuli.[1] A DHBC is generally composed of two blocks with different chemical natures where one block is hydrophilic and the other block is stimuli-responsive. When various types of external stimuli such as temperature,[2,3] pH,[4,5] and light[6] are applied, DHBCs become amphiphiles by switching the hydrophilic character of the stimuli-responsive block to hydrophobic, which induces reversible self-assembly into micelles or vesicles in aqueous solution.[7,8] Of special interest are thermoresponsive polymers whose solubility depends on temperature, since temperature is a simple external trigger for achieving reversible solvation and desolvation, which in turn leads to conformational changes. These polymers are soluble in aqueous solution below their lower critical solution temperature (LCST) through hydrogen bonding with water molecules, but become dehydrated and insoluble when heated above the LCST, resulting in abrupt phase separation.[9–13] Dendrimers are repeatedly branched, three-dimensional molecules with structural perfection.[14] Due to their precise architecture as well as highly functional periphery, dendrimers are very promising materials for biomedical applications such as drug and gene delivery.[15,16] While numerous architectures of block copolymers have been reported, most studies were focused on DHBCs with a linear–linear block structure due to their facile synthetic accessibility; however, the introduction of a dendritic structure as one component of a building block of DHBCs is particularly attractive since the aggregated morphologies can be further tuned through precise manipulation of dendritic structures.[17–23] Furthermore, linear–dendritic block copolymers allow one to take advantage of dendritic multivalency to create functional exteriors with high ligand densities for targeted drug delivery while keeping the phase segregated morphological behavior of traditional block copolymers.[24,25]

In this communication, we demonstrate that an entirely PEO-based biocompatible linear–dendritic block copolymer with a thermoresponsive linear block and a hydrophilic dendritic block can self-assemble into polymeric micelles by simply heating to a temperature above the LCST of the thermoresponsive linear block. The resulting polymeric micelles can be completely disrupted into unimers upon cooling to a temperature below its LCST and regenerated upon heating again. The entire process is depicted schematically in Scheme 1a.

The strategy employed in this study is schematically illustrated in Scheme 1b. A double-hydrophilic linear–dendritic block copolymer was synthesized based on poly(2-(2′-methoxyethoxy)ethyl methacrylate) (PMEO2MA) as a temperature responsive linear block and a multivalent hydrophilic polyester dendron block modified with poly(ethylene glycol). As shown in Scheme 1b, the dendritic initiator, B16Br **2** was synthesized by the reaction between the dendritic acid, B16COOH **1** and 2-hydroxyethyl bromoisobutyrate. Following this, the PMEO2MA-extended dendron, PMEO2MA-*b*-B16 **3** was prepared by atom transfer radical polymerization (ATRP)[26] from B16Br **2**. This polymerization was carried out in 50 vol% of anisole to MEO2MA, and in the presence of CuBr and 4,4′-bis(5-nonyl)-2,2′-bipyridine (dNbpy) as a

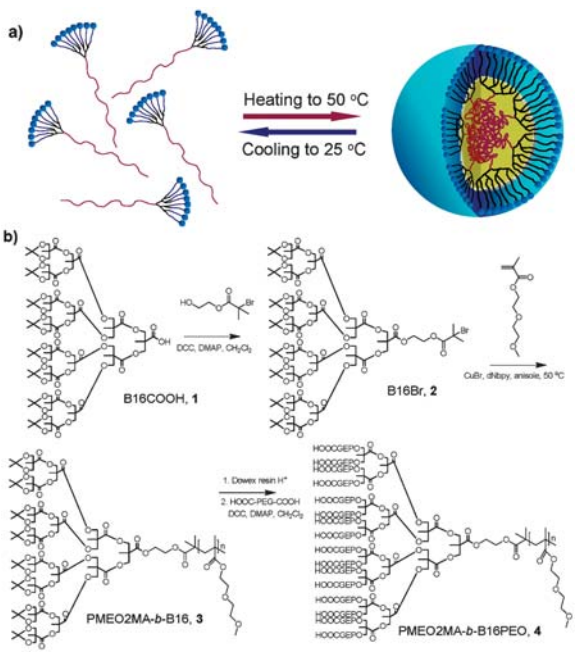

Scheme 1 (a) Schematic representation of reversible formation and disruption of the linear–dendritic polymeric micelles triggered by temperature. (b) The synthetic route toward the temperature-responsive linear–dendritic block copolymer, PMEO2MA-*b*-B16PEO **4**.

Department of Chemical Engineering, Massachusetts Institute of Technology, Cambridge, Massachusetts 02139, USA. E-mail: hammond@mit.edu

† Electronic supplementary information (ESI) available: Experimental details and additional AFM images. See DOI: 10.1039/b807561a

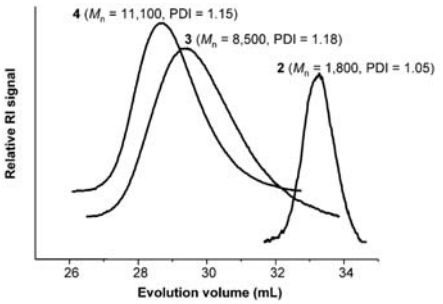

Fig. 1 GPC traces of B16Br **2**, PMEO2MA-*b*-B16 **3**, and PMEO2MA-*b*-B16PEO **4**.

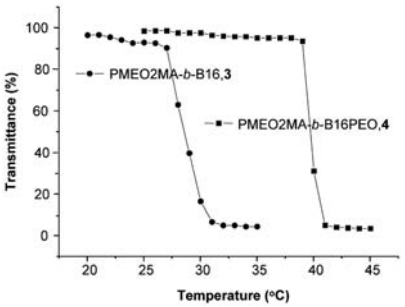

Fig. 2 Plot of transmittance as a function of temperature (600 nm, 1.0 °C min^{-1}) measured for aqueous solutions (10 mg mL^{-1}) of PMEO2MA-*b*-B16 **3** and PMEO2MA-*b*-B16PEO **4**.

catalyst. The [MEO2MA] : [B16Br **2**] ratio was fixed at 100 : 1. The polymerization was stopped when monomer conversion reached 40%. Finally, after deprotection of the acetonide groups of **3** by Dowex H^+ resin, the resulting hydroxyl groups were reacted with an excess of bis(carboxymethyl) ether (HOOC-PEG-COOH, MW = 600 g mol^{-1}) to give the linear–dendritic block copolymer, PMEO2MA-*b*-B16PEO **4**.

The molecular weight and molecular weight distribution of the reaction products **2**, **3**, and **4** were obtained by gel permeation chromatography (GPC) in tetrahydrofuran (THF) with conventional calibration based on polystyrene standards. Fig. 1 shows the GPC curves of B16Br **2** (M_n = 1800 g mol^{-1}; PDI = 1.05), PMEO2MA-*b*-B16 **3** (M_n = 8500 g mol^{-1}; PDI = 1.18), and PMEO2MA-*b*-B16PEO **4** (M_n = 11 100 g mol^{-1}; PDI = 1.15) (data shown in Table 1). A shift to higher molecular weight was observed after each chain extension step. The correlation between theoretical and experimental M_n values was excellent for PMEO2MA-*b*-B16 **3**, demonstrating the controlled nature of the polymerization. For PMEO2MA-*b*-B16PEO **4**, however, apparent M_n was much smaller than theoretical M_n. This result is common for globular, compact molecules such as dendrimers and molecular brushes since the hydrodynamic volume is lower than linear polymers with equivalent molecular weight, giving a smaller apparent molecular weight.[27,28]

Fig. 2 shows the values of LCST obtained for aqueous solutions of PMEO2MA-*b*-B16 **3** and PMEO2MA-*b*-B16PEO **4** (concentration was 10 mg mL^{-1}). For PMEO2MA-*b*-B16 **3**, a LCST of 28 °C was observed, which was the same as the previously reported value for the homopolymer PMEO2MA.[9] The LCST of PMEO2MA-*b*-B16PEO **4** increased to 39 °C with the addition of hydrophilic PEG segments. All results are summarized in Table 1.

The temperature-triggered formation, disruption, and regeneration of the polymeric micelles were confirmed by atomic force microscopy (AFM, Fig. 3; ESI†) prepared from an aqueous solution at a concentration of 1.0 mg mL^{-1}. This initial aqueous solution of PMEO2MA-*b*-B16PEO **4** was stirred continuously at 50 °C for 12 h before spin-coating onto silicon wafer for AFM analysis. The AFM images of the sample deposited after micellization at 50 °C revealed the presence of uniform, well dispersed individual globular species (micelles, Fig. 3a) with an average diameter of 24.8 ± 4.3 nm. After allowing the aqueous solution to cool down to 25 °C, a sample was taken again for AFM analysis. The previous well-defined globular micelles gave way to molecularly resolved individual polymer chains that could not be directly imaged with the AFM tips (Fig. 3b). This observation was consistent with the disruption of polymeric micelles by lowering the

Table 1 GPC results and LCST data for B16Br **2**, PMEO2MA-*b*-B16 **3** and PMEO2MA-*b*-B16PEO **4**

Entry	Conv (%)[a]	$M_{n,\,app}$[b]	M_w/M_n[b]	$M_{n,\,theo}$	$DP_{n,\,theo}$[d]	LCST[e]
2	—	1800	1.05	2275	—	—
3	40	8500	1.18	9795[c]	40	28
4	—	11 100	1.15	19 075	40	39

[a] Monomer conversion as determined by ^{1}H NMR spectroscopy for the ATRP of MEO2MA ([MEO2MA] : [B16Br **2**] : [CuBr] : [dNbpy] = 100 : 1 : 1 : 2, 50 vol% anisole, T = 50 °C). [b] Determined by GPC in THF. [c] $M_{n,theo}$ = monomer conversion × MW_{MEO2MA} × $[MEO2MA]_0/[B16Br\ 2]_0$ + $MW_{B16Br\ 2}$. [d] DP (degree of polymerization) of the linear block calculated by monomer conversion. [e] LCST as determined by UV-Vis spectroscopy by measuring % transmittance at 600 nm for the aqueous solution with a concentration of 10 mg mL^{-1}.

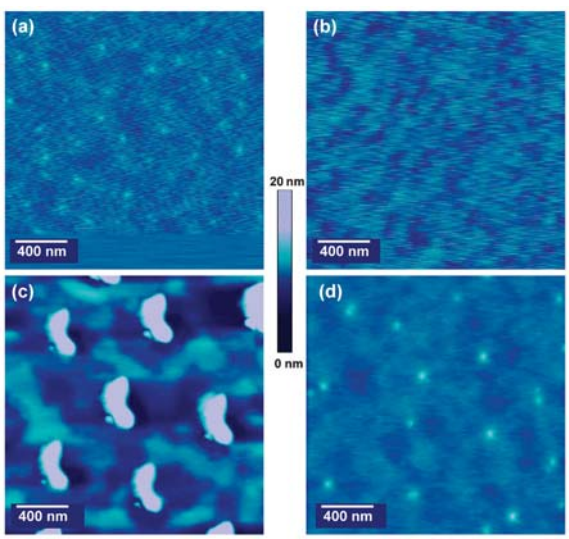

Fig. 3 AFM phase images of PMEO2MA-*b*-B16PEO **4** solutions spin-coated on a silicon wafer under various conditions: (a) the original micelles of PMEO2MA-*b*-B16PEO **4** at 50 °C; (b) the disrupted micelles after cooling to 25 °C; (c) the regenerated micelles after heating to 50 °C for 1 min; (d) the regenerated micelles after continuous heating at 50 °C for 120 min.

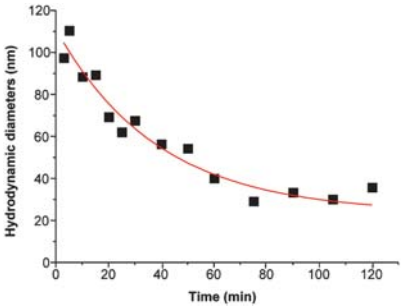

Fig. 4 Plot of hydrodynamic diameter distributions of the regenerated micelles as a function of time.

temperature below the LCST of PMEO2MA. The same solution at 25 °C was then re-heated to 50 °C. After time points of 1 min, 60 min, and 120 min, samples were taken and quickly spin-coated onto a silicon wafer. An AFM image of the sample deposited immediately after 1 min showed the presence of kinetically-controlled large aggregates (Fig. 3c). Continuous heating at 50 °C for 120 min induced thermodynamically stable micelles with an average diameter of 43.2 ± 6.1 nm, shown in Fig. 3d (see also ESI for the AFM image for 60 min†). The observed evolution of the morphology of the micelles can be explained by the annealing/equilibration effect accompanying the regeneration process.[6]

Dynamic light scattering (DLS) was conducted using photon correlation spectroscopy[18] in order to correlate with AFM results, which illustrate the micellar regeneration process *via* observation of micelles in the dry state. The average hydrodynamic diameter of the original micelles was 40 nm. For the disrupted micelles, however, the autocorrelation functions were not obtainable, proving the disruption of the micelles upon decrease of temperature. The apparent hydrodynamic diameters (CONTIN plot)[3] were measured as a function of time at 50 °C during the regeneration process of the micelles. All the autocorrelation functions showed single exponential decays, representing narrowly dispersed populations of particle sizes. As shown in Fig. 4, the hydrodynamic diameters of the micelles continuously decreased from 110 to 30 nm at 50 °C for 120 min, which indicates that the initial kinetically-controlled large aggregates eventually partition into thermodynamically-stable individual micelles.

In conclusion, we have shown that the double-hydrophilic linear–dendritic block copolymer, PMEO2MA-*b*-B16PEO, undergoes a reversible thermal transition which is accompanied by transformation between a double-hydrophilic and an amphiphilic linear–dendritic block copolymer. Consequently, polymeric micelles formed from an aqueous solution of PMEO2MA-*b*-B16PEO at 50 °C were disrupted by cooling down to 25 °C and regenerated by heating to 50 °C. This entire PEO-based biocompatible linear–dendritic copolymer is currently being investigated for temperature-induced controlled release of therapeutic agents as well as for active targeting by subsequent functionalization of the peripheral acid groups with biospecific ligands.

This work was financially supported by the National Institutes of Health (NIH), the MIT center for Cancer Nanotechnology Excellence, MIT Portugal Program, and National Science Foundation (NSF).

Notes and references

1 H. Colfen, *Macromol. Rapid Commun.*, 2001, **22**, 219.
2 P. De, S. R. Gondi and B. S. Sumerlin, *Biomacromolecules*, 2008, **9**, 1064.
3 X. Andre, M. Zhang and A. H. E. Mueller, *Macromol. Rapid Commun.*, 2005, **26**, 558.
4 C. M. Schilli, M. Zhang, E. Rizzardo, S. H. Thang, Y. K. Chong, K. Edwards, G. Karlsson and A. H. E. Mueller, *Macromolecules*, 2004, **37**, 7861.
5 J. Rodriguez-Hernandez and S. Lecommandoux, *J. Am. Chem. Soc.*, 2005, **127**, 2026.
6 H.-i. Lee, W. Wu, J. K. Oh, L. Mueller, G. Sherwood, L. Peteanu, T. Kowalewski and K. Matyjaszewski, *Angew. Chem., Int. Ed.*, 2007, **46**, 2453.
7 R. Haag, *Angew. Chem., Int. Ed.*, 2004, **43**, 278.
8 D. A. Rider, M. A. Winnik and I. Manners, *Chem. Commun.*, 2007, 4483.
9 J.-F. Lutz and A. Hoth, *Macromolecules*, 2006, **39**, 893.
10 H.-i. Lee, J. Pietrasik and K. Matyjaszewski, *Macromolecules*, 2006, **39**, 3914.
11 A. Munoz-Bonilla, M. Fernandez-Garcia and D. M. Haddleton, *Soft Matter*, 2007, **3**, 725.
12 J.-F. Lutz, O. Akdemir and A. Hoth, *J. Am. Chem. Soc.*, 2006, **128**, 13046.
13 J.-F. Lutz, *J. Polym. Sci., Part A: Polym. Chem.*, 2008, **46**, 3459.
14 O. A. Matthews, A. N. Shipway and J. F. Stoddart, *Prog. Polym. Sci.*, 1998, **23**, 1.
15 S. Svenson and A. Tomalia Donald, *Adv. Drug Delivery Rev.*, 2005, **57**, 2106.
16 M. W. Grinstaff, *Chem.–Eur. J.*, 2002, **8**, 2838.
17 L. Tian, P. Nguyen and P. T. Hammond, *Chem. Commun.*, 2006, 3489.
18 L. Tian and P. T. Hammond, *Chem. Mater.*, 2006, **18**, 3976.
19 K. R. Lambrych and I. Gitsov, *Macromolecules*, 2003, **36**, 1068.
20 I. Gitsov, A. Simonyan and N. G. Vladimirov, *J. Polym. Sci., Part A: Polym. Chem.*, 2007, **45**, 5136.
21 B.-K. Cho, A. Jain, S. Mahajan, H. Ow, S. M. Gruner and U. Wiesner, *J. Am. Chem. Soc.*, 2004, **126**, 4070.
22 E. R. Gillies, T. B. Jonsson and J. M. J. Frechet, *J. Am. Chem. Soc.*, 2004, **126**, 11936.
23 J. L. Mynar, A. P. Goodwin, J. A. Cohen, Y. Ma, G. R. Fleming and J. M. J. Frechet, *Chem. Commun.*, 2007, 2081.
24 T. C. Stover, Y. S. Kim, T. L. Lowe and M. Kester, *Biomaterials*, 2007, **29**, 359.
25 C. M. B. Santini, T. A. Hatton and P. T. Hammond, *Langmuir*, 2006, **22**, 7487.
26 J.-S. Wang and K. Matyjaszewski, *J. Am. Chem. Soc.*, 1995, **117**, 5614.
27 B. S. Sumerlin, D. Neugebauer and K. Matyjaszewski, *Macromolecules*, 2005, **38**, 702.
28 Q. Zheng and C.-y. Pan, *Macromolecules*, 2005, **38**, 6841.

